Role of the Carboxy-Terminal Region of the GluRε2 Subunit in Synaptic Localization of the NMDA Receptor Channel

Hisashi Mori,[1] Toshiya Manabe,[2]
Masahiko Watanabe,[3] Yasushi Satoh,[1,6]
Norimitsu Suzuki,[2] Shima Toki,[3]
Kazuhiro Nakamura,[1,6] Takeshi Yagi,[4,6]
Etsuko Kushiya,[5] Tomoyuki Takahashi,[2]
Yoshiro Inoue,[3] Kenji Sakimura,[5,6]
and Masayoshi Mishina[1,4,6,7]
[1] Department of Molecular Neurobiology
and Pharmacology
[2] Department of Neurophysiology
School of Medicine
University of Tokyo
Tokyo 113-0033
[3] Department of Anatomy
Hokkaido University
School of Medicine
Sapporo 060-8638
[4] Laboratory of Neurobiology and Behavioral Genetics
National Institute for Physiological Science
Okazaki 444-0867
[5] Department of Cellular Neurobiology
Brain Research Institute
Niigata University
Niigata 951-8585
[6] Core Research for Evolutional Science and Technology
Japan Science and Technology Corporation
Saitama 332-0012
Japan

Summary

The synaptic localization of the N-methyl-D-aspartate (NMDA) type glutamate receptor (GluR) channel is a prerequisite for synaptic plasticity in the brain. We generated mutant mice carrying the carboxy-terminal truncated GluRε2 subunit of the NMDA receptor channel. The mutant mice died neonatally and failed to form barrelette structures in the brainstem. The mutation greatly decreased the NMDA receptor–mediated component of hippocampal excitatory postsynaptic potentials and punctate immunofluorescent labelings of GluRε2 protein in the neuropil regions, while GluRε2 protein expression was comparable. Immunostaining of cultured cerebral neurons showed the reduced punctate staining of the truncated GluRε2 protein at synapses. These results suggest that the carboxy-terminal region of the GluRε2 subunit is important for efficient clustering and synaptic localization of the NMDA receptor channel.

Introduction

The N-methyl-D-aspartate (NMDA) subtype of the glutamate receptor (GluR) channel plays roles in synaptic plasticity as a molecular coincidence detector and in neuronal pattern formation during development (Cline et al., 1987; Kleinschmidt et al., 1987; Bliss and Collingridge, 1993; Malenka and Nicoll, 1993). Combinations of the GluRε (NR2) and GluRζ (NR1) subunits constitute NMDA receptor channels (Kutsuwada et al., 1992; Meguro et al., 1992; Monyer et al., 1992). There are four GluRε subunit genes (Ikeda et al., 1992; Kutsuwada et al., 1992; Meguro et al., 1992; Monyer et al., 1992; Nagasawa et al., 1996), while the GluRζ subunit variants are derived from a single gene (Moriyoshi et al., 1991; Sugihara et al., 1992; Yamazaki et al., 1992; Hollmann et al., 1993). At the embryonic stages, GluRε2 (NR2B) mRNA is expressed in the entire brain, and GluRε4 (NR2D) mRNA is expressed in the diencephalon and brainstem (Watanabe et al., 1992, 1993; Akazawa et al., 1994; Monyer et al., 1994). After birth, GluRε1 (NR2A) mRNA appears in the entire brain, and GluRε3 (NR2C) mRNA appears mainly in the cerebellum. The expression of GluRε2 mRNA becomes restricted to the forebrain and that of GluRε4 mRNA is strongly reduced. GluRζ1 mRNA is found ubiquitously in the brain during development. The four GluRε subunits are also distinct in functional properties and regulations (Seeburg, 1993; Mori and Mishina, 1995). Thus, the molecular compositions and functional properties of NMDA receptor channels are different, depending on the brain regions and developmental stages, and multiple GluRε subunits are major determinants of NMDA receptor channel diversity.

We examined the physiological significance of NMDA receptor channel diversity by gene targeting. The disruption of the GluRε1 gene resulted in the reduction of hippocampal long-term potentiation (LTP) and impairment of Morris water maze and contextual learning (Sakimura et al., 1995; Kiyama et al., 1998). GluRε2 mutant mice died shortly after birth and failed to form the whisker-related neural pattern (barrelettes) in the brainstem trigeminal complex (Kutsuwada et al., 1996), similar to GluRζ1 mutant mice (Forrest et al., 1994; Li et al., 1994). The ablation of the GluRε2 subunit also impaired synaptic plasticity in the hippocampus (Kutsuwada et al., 1996; Ito et al., 1997). GluRε4 mutant mice exhibited reduced spontaneous activity (Ikeda et al., 1995), while GluRε3 mutant mice showed little obvious deficit (Ebralidze et al., 1996; Kadotani et al., 1996; Sprengel et al., 1998).

The GluRε subunits of the NMDA receptor channel have large carboxy-terminal domains (Ikeda et al., 1992; Kutsuwada et al., 1992; Meguro et al., 1992; Monyer et al., 1992). These putative cytoplasmic regions contain the interaction sites with the PSD-95 (postsynaptic density–95) family of PDZ domain–containing proteins and α-actinin (Kornau et al., 1995; Kim et al., 1996; Müller et al., 1996; Niethammer et al., 1996; Wyszynski et al., 1997). The carboxy-terminal region of the GluRε2 subunit is responsible for the modulation of NMDA receptor channels by a protein kinase C activator (Mori et al., 1993) and is phosphorylated by Ca^{2+}/calmodulin-dependent protein kinase II (CaMKII) (Omkumar et al., 1996). GluRε2 protein is one of the most strongly tyrosine-phosphorylated proteins among postsynaptic density proteins (Moon et al., 1994). To investigate the physiological roles of the region, we have generated mutant

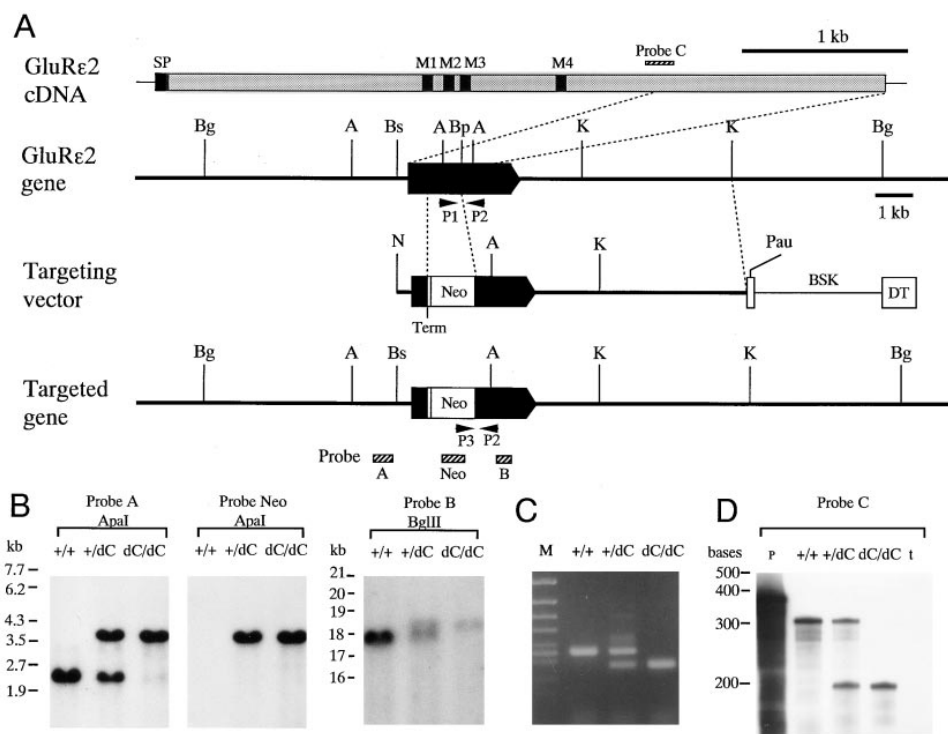[7] To whom correspondence should be addressed.

Figure 1. Generation of *GluRε2dC* Mutant Mice by Homologous Recombination in TT2 ES Cells

(A) Schematic representations of *GluRε2* cDNA, the *GluRε2* gene, targeting vector, and targeted gene. Abbreviations: BSK, plasmid pBluescript; DT, diphtheria toxin gene; M1–M4, four hydrophobic segments; Neo, neomycin phosphotransferase gene; Pau, mRNA-destabilizing and transcription-pausing signals; Term, translational termination codon; SP, signal peptide; A, ApaI; Bg, BglII; Bp, Bpu1102I; Bs, BspHI; K, KpnI; N, NotI. Hatched bars indicate the location of probes for Southern blot analysis (Probes A and B and Neo) and RNase protection assay (Probe C), and arrowheads indicate PCR primers (P1, P2, and P3).
(B) Southern blot analysis of ApaI- or BglII-digested genomic DNA of wild-type (+/+), heterozygous (+/dC), and homozygous (dC/dC) mice.
(C) Agarose gel electrophoresis of DNA fragments amplified with PCR from wild-type (+/+), heterozygous (+/dC), and homozygous (dC/dC) mice. The amplified DNA fragments derived from the wild-type and mutated *GluRε2* genes were 350 bp and 276 bp, respectively. Lane M, HincII-digested ΦX174 DNA as size markers.
(D) RNase protection analysis of *GluRε2* and *GluRε2dC* mRNAs in the whole brain of mice at P0. Positions of RNA century markers (bases) are shown on the left. The sizes of the protected RNA by wild-type and mutant mRNAs were 303 bases and 201 bases, respectively. Abbreviations: p, ^{32}P-labeled antisense RNA probe C; t, control yeast tRNA.

mice carrying a carboxy-terminal deletion of the GluRε2 subunit. In contrast to the recent argument by Sprengel et al. (1998), we have found that the carboxy-terminal truncation disturbs the synaptic localization of the functional NMDA receptor channels.

Results

Mutant Mice Expressing the Truncated GluRε2 Subunit

The carboxy-terminal region of the GluRε2 subunit was responsible for the augmentation of GluRε2/GluRζ1 NMDA receptor channel activity by 12-O-tetradecanoyl-phorbol-13-acetate (TPA) treatment in a *Xenopus laevis* oocyte expression system (Mori et al., 1993). The deletion of about two-thirds of this region (459 of 644 amino acids) of the GluRε2 subunit (GluRε2dC) eliminated the augmentation by TPA without abolishing the channel activity (data not shown). To investigate the physiological roles of the carboxy-terminal region in vivo, we generated mutant mice that expressed the truncated GluRε2dC subunit by homologous recombination in embryonic

stem (ES) cells (Figures 1A–1C). The targeting vector carried a translational termination codon after the Leu-997 codon of the *GluRε2* gene and a replacement of the following 0.9 kb coding region by an SV40 poly(A) addition signal and neomycin phosphotransferase gene (Figure 1A).

No homozygous mutant mice were found in 434 offspring after weaning. Among 167 newborn pups, however, there were 42 wild-type (+/+), 83 heterozygous (+/dC), and 42 homozygous (dC/dC) mice, the ratio being close to 1:2:1. The proportion of the mutant mice gradually reduced, and no homozygous *GluRε2dC* mice were found at postnatal day 3 (P3). The mutant mice were recovered by hand feeding, as reported for the *GluRε2* subunit null mutant mice (Kutsuwada et al., 1996). When reared by hand feeding, postnatal days are referred to with asterisks (e.g., P2* represents postnatal day 2, reared by hand feeding).

Expression of GluRε2dC Protein

RNase protection analysis of total brain RNA of mice at P0 showed that the expression level of the mutant
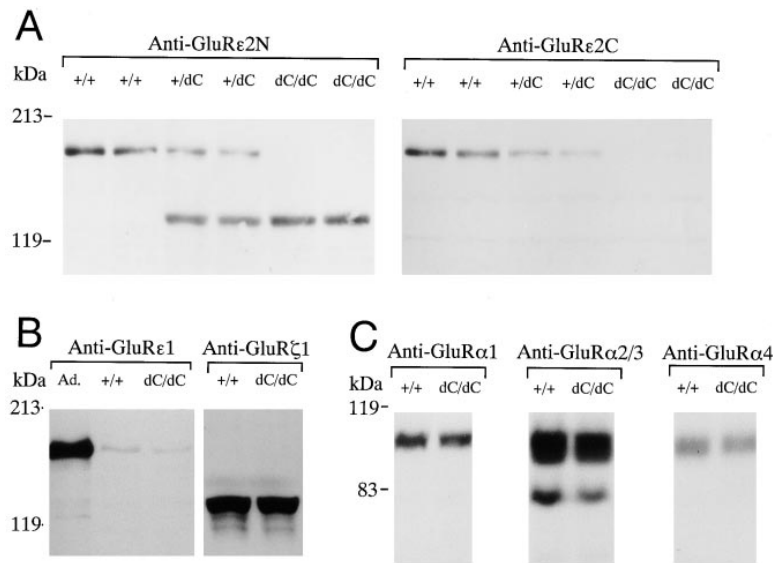
Figure 2. Expression of GluR Channel Subunit Proteins in the Brain

Western blot analyses of the whole brain proteins of wild-type (+/+), heterozygous (+/dC), and homozygous (dC/dC) mice at P0 with anti-GluRε2N and anti-GluRε2C (A), anti-GluRε1 and anti-GluRζ1 (B), and anti-GluRα1, anti-GluRα2/3, and anti-GluRα4 (C). Samples from two mice of each genotype were presented in (A). Abbreviation: Ad, adult wild-type mice.

GluRε2dC mRNA was comparable to that of the wild-type GluRε2 mRNA (Figure 1D). Anti-GluRε2N antibody against the amino-terminal region of the GluRε2 subunit (Watanabe et al., 1998) detected ∼130 kDa truncated GluRε2dC protein and ∼180 kDa wild-type GluRε2 protein in the brains of mutant and wild-type mice at P0, respectively (Figure 2A). The difference in size (∼50 kDa) corresponded well to the value estimated from the deleted region (459 amino acids). The amount of GluRε2dC protein in the mutant mice was comparable to that of GluRε2 protein in the wild-type mice. Anti-GluRε2C antibody against the carboxy-terminal region of the GluRε2 subunit (Watanabe et al., 1998) detected ∼180 kDa GluRε2 protein but no 130 kDa protein as expected (Figure 2A). The carboxy-terminal truncation of the GluRε2 subunit did not appreciably affect the expression of the NMDA-type GluR channel subunits GluRε1 and GluRζ1 (Figure 2B); the α-amino-3-hydroxy-5-methyl-4-isoxazole propionic acid (AMPA) type GluR channel subunits GluRα1 (GluR1), GluRα2/GluRα3 (GluR2/3), and GluRα4 (GluR4) (Figure 2C); or neuron-specific enolase, a marker protein of neurons (Schmechel et al., 1978) (data not shown). The expression of GluRε1 protein was faint as compared with that of the adult mice (Figure 2B).

NMDA Receptor Channel–Mediated EPSPs in the Hippocampus

There was no clear difference in the basic properties of non-NMDA receptor channel–mediated excitatory postsynaptic potentials (EPSPs) in the CA1 region of hippocampal slices between the wild-type (n = 5) and GluRε2dC (n = 7) mice at P1*–P3* (Figure 3). Input–output relationships of AMPA receptor channel–mediated synaptic responses estimated by measuring the ratio of EPSPs to fiber volley amplitudes were indistinguishable between the wild-type (5.2 ± 1.1, mean ± SEM, n = 5) and mutant (4.5 ± 0.8, n = 7) mice (t test, p > 0.3), suggesting that the amount of AMPA receptor channels at the mutant synapse was not altered. We measured NMDA receptor channel–mediated EPSPs in

a Mg^{2+}-free medium containing 10 µM 6-cyano-7-nitro-qunoxaline-2,3-dione (CNQX), which was completely abolished by 50 µM D-2-amino-5-phosphonovalerate (D-APV). The ratio of NMDA components to non-NMDA components of EPSPs in the mutant slices (8.9% ± 2.3%, n = 7) was much lower than that of the wild-type slices (32.2% ± 7.6%, n = 5) (Figure 3) (t test, p < 0.05). The ratio of NMDA receptor channel–mediated synaptic responses to fiber volley amplitudes in the mutant mice (0.41 ± 0.13, n = 7) was also significantly smaller than that of the wild-type mice (1.90 ± 0.73, n = 5) (t test, p < 0.02).

To examine whether the strong reduction of NMDA receptor channel–mediated EPSPs in GluRε2dC mice is due to the decrease in the amounts of synaptic NMDA receptor channels or the alteration of the channel properties, we analyzed the single channel properties of NMDA-induced currents in outside-out patches excised from pyramidal cells in the hippocampal CA1 region of wild-type and mutant mice at P1*. The main single channel conductances of NMDA-gated channels measured at −80 mV were 46.4 ± 0.05 pS in the wild-type cells (n = 6; Figure 4A) and 46.7 ± 0.08 pS in the mutant cells (n = 6; Figure 4B). The mean open times of NMDA-gated channels were 2.43 ± 0.14 ms in the wild-type cells (n = 6; Figure 4C) and 2.23 ± 0.14 ms in the mutant cells (n = 6; Figure 4D). Thus, there was no significant difference in the single channel properties of the NMDA receptor channels between the wild-type and mutant cells (t test, p = 0.41 and 0.21 for the conductance and mean open time, respectively). We also measured these parameters at different membrane potentials ranging from −60 mV to +80 mV and obtained qualitatively similar results to those at −80 mV. Furthermore, the reversal potential estimated by the linear regression fitting of the single channel current–voltage relationship was not significantly different between the wild-type (−8.6 ± 1.9 mV, n = 4) and mutant (−4.3 ± 2.6 mV, n = 4) mice (t test, p > 0.1). These results suggest that the amounts of functional synaptic NMDA receptor channels were decreased in the hippocampal CA1 region of GluRε2dC

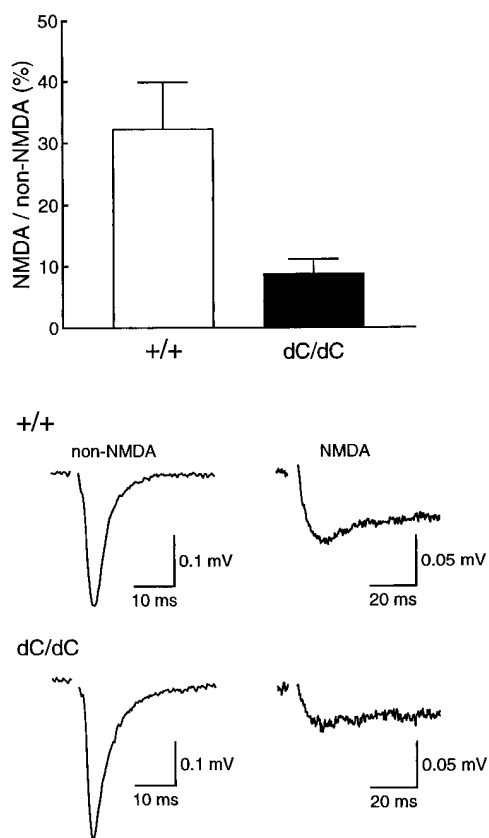Figure 3. NMDA Receptor Channel–Mediated Responses in the CA1 Subfield of the Hippocampus

Ratio of the amplitudes of the NMDA receptor channel–mediated component to those of the non-NMDA receptor channel–mediated components of EPSPs in wild-type (+/+) and mutant (dC/dC) hippocampal slices from mice at P1*–P3*. Traces represent averages of 10 consecutive EPSPs recorded in a slice from the wild-type or mutant mouse at P2*.

mice without any change in the voltage dependence at the single channel level.

Localization of GluRε2dC Protein

We examined immunohistochemically the localization of GluRε2dC protein by using a novel protease pretreatment procedure developed by Watanabe et al. (1998), since conventional methods failed to detect specific signals of the NMDA receptor channel subunits in histological brain sections, as judged from the comparison of the stained sections prepared from the wild-type mice with those of mutant mice lacking the respective subunits of the NMDA receptor channel. Hippocampal sections from wild-type, GluRε2dC, and GluRε2 null mutant (−/−) mice at P2* were double labeled with anti-GluRε2N and anti-synaptophysin antibodies (Figure 5). In the wild-type mice, we detected high levels of immunofluorescent signals specific to GluRε2 protein in the hippocampal CA1 region (Figures 5A and 5B). The signals were observed as punctate labelings concentrated above and beneath the pyramidal cell layer, i.e., in neuropil layers where dendritic spines of pyramidal cells form excitatory synapses. Many puncta were apposed

to puncta labeled for synaptophysin, a presynaptic marker protein (Buckley et al., 1987), and yielded a fused yellow-colored interface between them, suggesting the postsynaptic localization of GluRε2 protein. There were also a considerable number of GluRε2-immunopositive puncta apart from any synaptophysin-immunopositive ones, which may represent protein clusters in transport or at immature synapses in the midst of active synaptogenesis (Aoki et al., 1994). In GluRε2 null mutant mice, there were comparable stainings for synaptophysin but no signals for GluRε2 protein (Figures 5E and 5F), indicating that the immunostaining signals with anti-GluRε2N antibody in the wild-type sections were authentic.

There were no significant differences in stainings for synaptophysin between the wild-type and GluRε2dC mutant mice at P2* (Figures 5A and 5C). On the other hand, the number and size of punctate labelings with anti-GluRε2N antibody in the neuropil of the hippocampus were reduced in GluRε2dC mutant mice (Figures 5C and 5D). Some of the GluRε2dC puncta were apposed to synaptophysin-immunopositive puncta, but their sizes were apparently smaller than the synaptophysin puncta. Furthermore, yellow-colored interface in the GluRε2dC mutant mice was smaller than that in the wild-type mice. These results suggest that the amount of synaptic GluRε2dC protein was decreased in GluRε2dC mutant mice.

To further examine the clustering and localization of GluRε2 protein at more mature stages, we analyzed cultured neurons (Figure 6). Cerebral neurons were prepared from wild-type, GluRε2dC, and GluRε2 null mutant mice at embryonic day 18 and were cultured for 7 days. Immunofluorecent staining for synaptophysin was comparable among cultured neurons from wild-type, GluRε2dC, and GluRε2 null mutant mice. GluRε2 clusters developed well in the wild-type neurons, and essentially all of them colocalized with synaptophysin, while there were no signals for GluRε2 protein in the neurons from GluRε2 null mutant mice, except for some nonspecific stainings in the soma. In neurons from GluRε2dC mutant mice, however, the number of GluRε2dC clusters was much less than that of GluRε2 clusters in the wild-type neurons (Figure 6A). Furthermore, some of the GluRε2dC clusters did not colocalize with synaptophysin (Figure 6B). These results suggest that carboxy-terminal truncation hinders the efficient clustering and synaptic localization of the GluRε2 subunit of the NMDA receptor channel. The formation and distribution of GluRα1 clusters were indistinguishable between neurons from wild-type and GluRε2dC mutant mice (Figure 6C).

Induction of Hippocampal LTD

Prolonged low frequency stimulation of afferent fibers produced robust long-term depression (LTD) in the CA1 region of the hippocampal slices prepared from wild-type mice at P2*–P3* (Figure 7, top), as reported previously (Kutsuwada et al., 1996). The EPSP amplitude 30 min after stimulation was 79.6% ± 0.6% (n = 3) of the control value. The low frequency stimulation induced LTD in two out of five hippocampal slices prepared from the mutant mice (Figure 7, middle) but failed in three

+/+   dC/dC

A   B   10 ms   2 p

(Histograms — panels A, C: Frequency vs −Amplitude (pA), 0–5; and Frequency vs Open time (ms), 0.1–100. Panels B, D: same axes for dC/dC.)
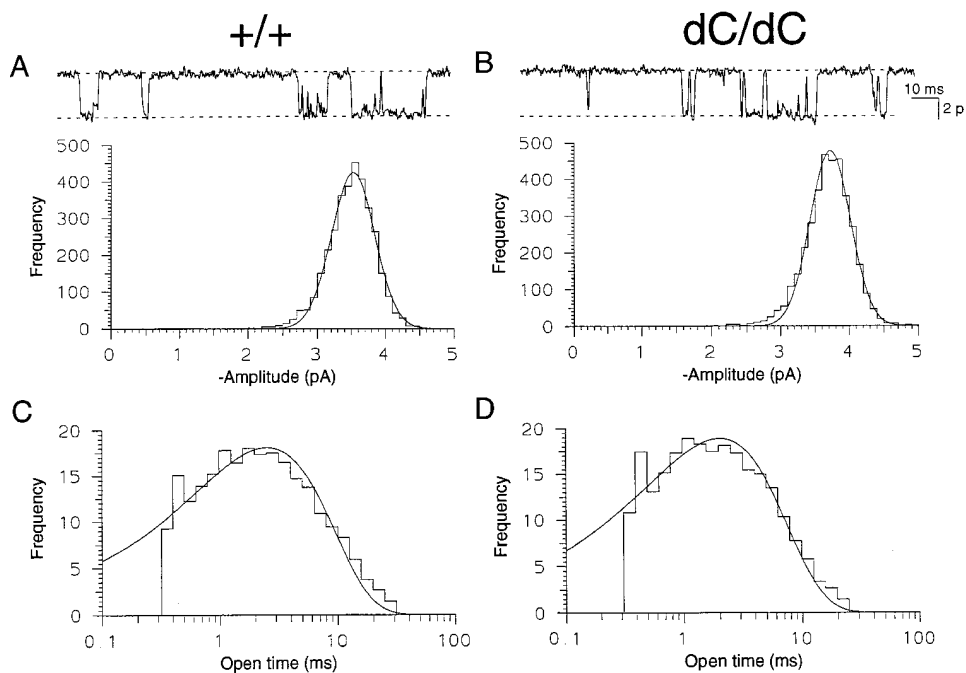
C   D

Figure 4. NMDA-Gated Single Channel Currents in Outside-Out Patches Excised from Hippocampal CA1 Pyramidal Cells of Wild-Type (+/+) and Mutant (dC/dC) Mice at P1*

Channel openings in a patch from wild-type (A) and mutant (B) mice are shown. Dashed lines in sample records (upper panel) indicate the mean current amplitude derived from the single channel amplitude distribution (histograms). Open time histograms are binned logarithmically, and a square root transformation of the ordinate (event per bin) is used. Histograms are fitted with single exponentials for wild-type (C) and mutant (D) cells.

slices (Figure 7, bottom). In two mutant slices, the EPSP amplitudes 30 min after stimulation were 76.3% and 79.3% of the control value, the extent of LTD being comparable to that of the wild-type slices. The ratios of the NMDA component to the non-NMDA component of EPSPs were 10.2% and 21.7% in the two mutant slices, which showed LTD induction, while the ratios were 4.2%, 7.5%, and 8.3% in the three mutant slices, which failed to exhibit LTD.

Neuronal Pattern Formation in the Brainstem
There was no abnormality in gross anatomical organization of the brain of GluRε2dC mice at P0 (data not shown). In the spinal tract nucleus of the brainstem trigeminal complex of wild-type mice at P2*, cytochrome oxidase histochemistry showed discrete neural repeating units called barrelettes corresponding to the whiskers (n = 16; Figure 8A). In contrast, the formation of chemoarchitectural barrelettes was impaired in mutant mice at P2* (n = 9; Figure 8B), as reported for GluRε2 mutant mice (Kutsuwada et al., 1996).

Discussion

In the present investigation, we examined the physiological role of the carboxy-terminal region of the GluRε2 subunit of the NMDA receptor channel in vivo by generating and analyzing mutant mice. The GluRε2 and GluRζ1 subunits are the main constituents of the functional NMDA receptor channels in the hippocampal CA1

region of the mouse brain at neonatal stages (Watanabe et al., 1992, 1993), and the contributions of the other GluRε subunits, if any, are negligible, since we found no synaptic NMDA receptor responses in the hippocampal CA1 region of the GluRε2 subunit null mutant mice at these stages (Kutsuwada et al., 1996). Thus, the hippocampal CA1 synapses at neonatal stages will be an ideal place to examine the effect of the carboxy-terminal truncation of the GluRε2 subunit on synaptic function.

Synaptic Localization
We found that the NMDA receptor channel–mediated components of EPSPs in the hippocampal CA1 region were strongly reduced in GluRε2dC mice, although the expression level of the truncated GluRε2dC protein was comparable to that of GluRε2 protein in wild-type mice. Furthermore, the immunohistochemical analyses with anti-GluRε2N antibody showed that punctate labelings of GluRε2dC protein in the neuropil of the hippocampus were reduced in the mutant mice, and that the amounts of the truncated GluRε2 subunit at the synapses were decreased in the cultured cerebral neurons prepared from the mutant mice. These results suggest that the carboxy-terminal truncation of the GluRε2 subunit exerts little effect on the expression of the subunit protein but does affect its efficient clustering and synaptic localization. It remains to be examined whether the clustering and synaptic localization are serial or separable steps, although the carboxy-terminal region appears to be important for both steps. It is likely that truncated GluRε2
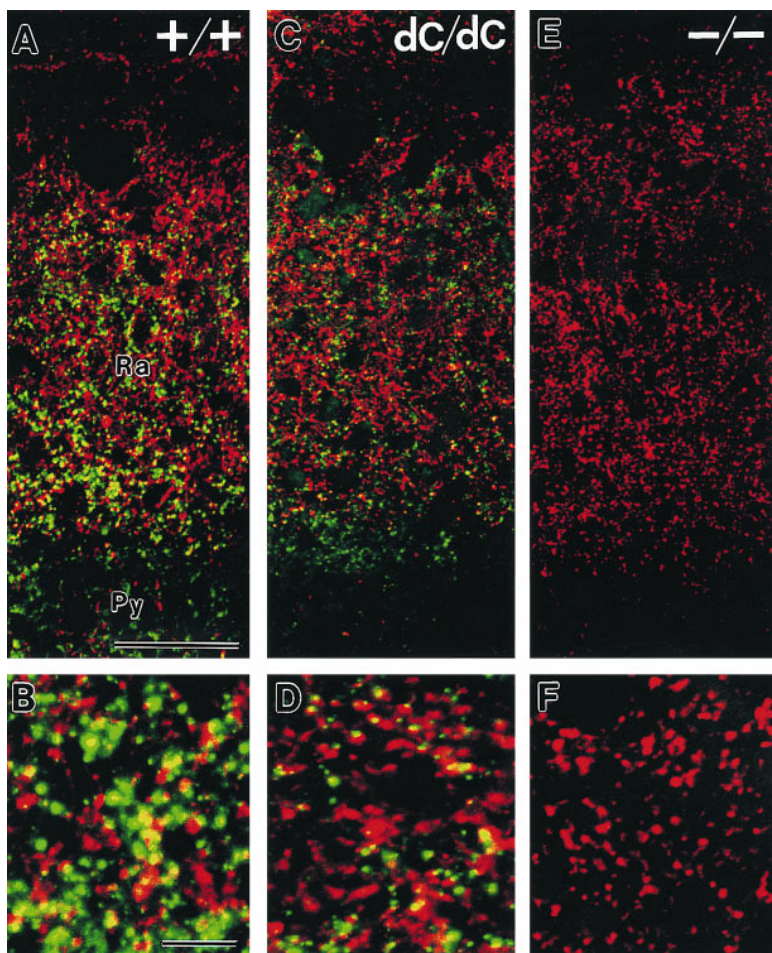
Figure 5. Immunohistochemical Localization of GluRε2 Subunit Protein

Double immunofluorescent staining with anti-GluRε2N (green) and anti-synaptophysin (red) antibodies of the hippocampal CA1 region of wild-type (A and B), *GluRε2dC* mutant (C and D), and *GluRε2* null mutant (E and F) mice at P2*. Abbreviations: Py, pyramidal cell layer; Ra, stratum radiatum. Scale bars, 50 μm in (A), 10 μm in (B).

proteins are present as complexes with the GluRζ1 subunit to form functional NMDA receptor channels in vivo, because the GluRε2 subunit is degraded in the absence of the GluRζ1 subunit (Forrest et al., 1994). Some GluRε2dC proteins that fail to form clusters in the mutant mice may be distributed diffusely and be immunohistochemically undetectable under our conditions. Consistent with this view, it was reported that muscle acetylcholine receptor proteins in MuSK-deficient mice were diffusely distributed and were histochemically undetectable though their expression level was normal (DeChiara et al., 1996).

The carboxy-terminal region of the GluRε2 subunit contains interaction sites with the PSD-95 family of PDZ domain–containing proteins, and this interaction has been suggested to be important for synaptic localization and clustering in vitro (Kornau et al., 1995; Kim et al., 1996; Müller et al., 1996; Niethammer et al., 1996). In view of the essential role of the PDZ domain–containing proteins in the proper subcellular localization of some membrane proteins in *Drosophila* and *Caenorhabditis elegans* (Simske et al., 1996; Chevesich et al., 1997; Tejedor et al., 1997), it is likely that the loss of GluRε2–PSD-95 family protein interactions by the carboxy-terminal deletion of the GluRε2 subunit resulted in the impairment of the efficient synaptic localization of the NMDA receptor channels in vivo. The fact that the carboxy-terminal truncation does not completely eliminate the synaptic localization of the GluRε2 subunit suggests the presence of additional mechanisms for synaptic localization of NMDA receptor channels. Some synaptic NMDA responses found in the hippocampus of the *GluRε2dC* mice might have resulted from synaptic localization through the interaction between certain GluRζ1 variants in heterooligomeric NMDA receptor channels and PSD-95 family proteins or α-actinin (Laurie and Seeburg, 1994; Kornau et al., 1995; Zhong et al., 1995; Wyszynski et al., 1997). In addition, the phosphorylation of the GluRζ1 subunit may also play a role in the clustering of NMDA receptor channels (Ehlers et al., 1995).

Consistent with our results, the deletion of almost the entire carboxy-terminal putative cytoplasmic region of the GluRε2 subunit resulted in the neonatal death of the mutant mice (Sprengel et al., 1998). On the other hand, Sprengel et al. (1998) argued that the GluRε2 subunit truncation impaired signal transduction rather than synaptic localization, in contrast to our conclusion. However, neither quantitative analyses of synaptic NMDA receptor channel responses nor immunohistochemical analyses of the localization of the truncated protein were presented. The large carboxy-terminal deletion of both the GluRε1 and GluRε3 subunits resulted in the degradation of GluRζ1 subunit protein as well as mutant proteins in the cerebellar granule cells (Sprengel et al., 1998), which may indicate the failure of proper clustering and localization of these proteins. In the hippocampus, the
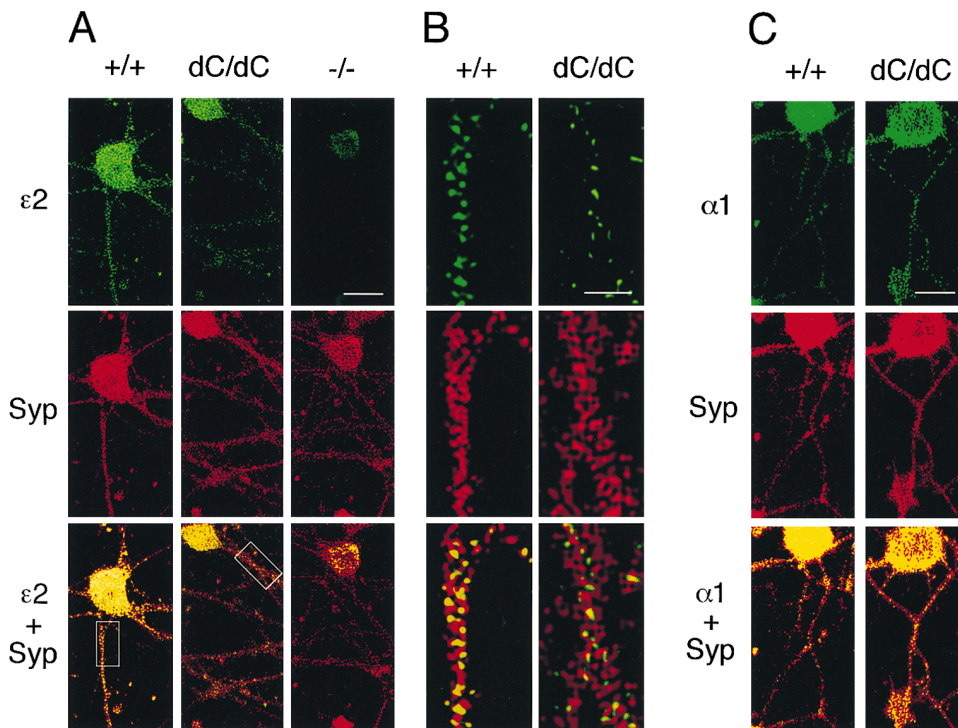
Figure 6. Double Immunofluorescent Staining of the Cultured Cerebral Neurons from Wild-Type (+/+), GluRε2dC Mutant (dC/dC), and GluRε2 Null Mutant (−/−) Mice

(A) Staining with anti-GluRε2N (ε2, green) and anti-synaptophysin (Syp, red) antibodies.
(B) Magnification of rectangular regions in (A).
(C) Staining with anti-GluRα1 (α1, green) and anti-synaptophysin (Syp, red) antibodies.
Scale bars, 20 μm in (A) and (C), 5 μm in (B).

synaptic localization of the truncated GluRε1 protein would be possible by forming complexes with the intact GluRε2 and GluRζ1 subunits. Thus, the studies of Sprengel et al. (1998) cannot exclude the importance of the carboxy-terminal region of the GluRε subunits in synaptic localization.

Synaptic Plasticity

At neonatal stages P2*–P3*, prolonged low frequency stimulation gives rise to homosynaptic LTD of excitatory synaptic transmission in the hippocampus, and this form of LTD is dependent on the NMDA receptor channel in our conditions (Kutsuwada et al., 1996). In the GluRε2dC mutant mice, some slices exhibited LTD comparable in magnitude to that of the wild-type slices, while the probability of hippocampal LTD induction appeared to be decreased. Thus, the carboxy-terminal region of the GluRε2 subunit is dispensable for LTD induction. The amount of transient Ca^{2+} influx through the NMDA receptor channel is critical for the induction of LTP or LTD in the adult hippocampal slices, as represented by the experiments using different concentrations of D-APV (Cummings et al., 1996). It is likely that the decreased synaptic localization of the NMDA receptor channels would result in the reduction of Ca^{2+} influx at the synapse, leading to the lower probability of LTD induction. The possibility remains that the deletion of the carboxy-terminal region may decrease the efficacy of signal transduction to induce synaptic plasticity by removing

the interaction sites with PSD-95 family proteins (Kornau et al., 1995; Kim et al., 1996; Müller et al., 1996; Niethammer et al., 1996) and/or the phosphorylation sites of various protein kinases (Mori et al., 1993; Moon et al., 1994; Omkumar et al., 1996).

Experimental Procedures

Generation of GluRε2dC Mutant Mice

A genomic DNA clone carrying the carboxy-terminal coding region of the GluRε2 gene was isolated from a C57BL/6 genomic library with the 121 bp BbsI fragment from the pGRU9 (Kutsuwada et al., 1992) as a probe. The translational termination codon TAG was inserted immediately after the Leu-997 codon of the GluRε2 gene, and the following 0.9 kb genomic coding region was replaced by a 1.4 kb DNA fragment composed of an SV40 poly(A) addition signal sequence from pMC1NeopA (Stratagene) and a phosphoglycerate kinase-1 gene promoter–driven neomycin phosphotransferase gene from pGK2Neo (Yagi et al., 1993b) that was flanked by loxP sequences (Sternberg et al., 1986). The targeting vector pTVE2DC contained 0.7 kb GluRε2 gene at the 5′ side and 7.1 kb GluRε2 gene at the 3′ side, followed by mRNA destabilizing and transcription-pausing signals (Pau) and an MC1 promoter–driven diphtheria toxin gene (DT) from pPauDT1 (Sakimura et al., 1995) (Figure 1).

TT2 ES cells derived from the F1 hybrid of C57BL/6 and CBA mice (Yagi et al., 1993a) were transfected with NotI-cleaved pTVE2DC by electroporation as described (Sakimura et al., 1995). A targeted clone was identified by G418 selection, PCR, and Southern blot hybridization. The recombinant ES cells were injected into eight-cell embryos of ICR mice to produce chimeras. A chimera was mated with C57BL/6 mice to yield F2 heterozygous mice with a genetic background of C57BL/6 (75%) and CBA (25%). Homozygous
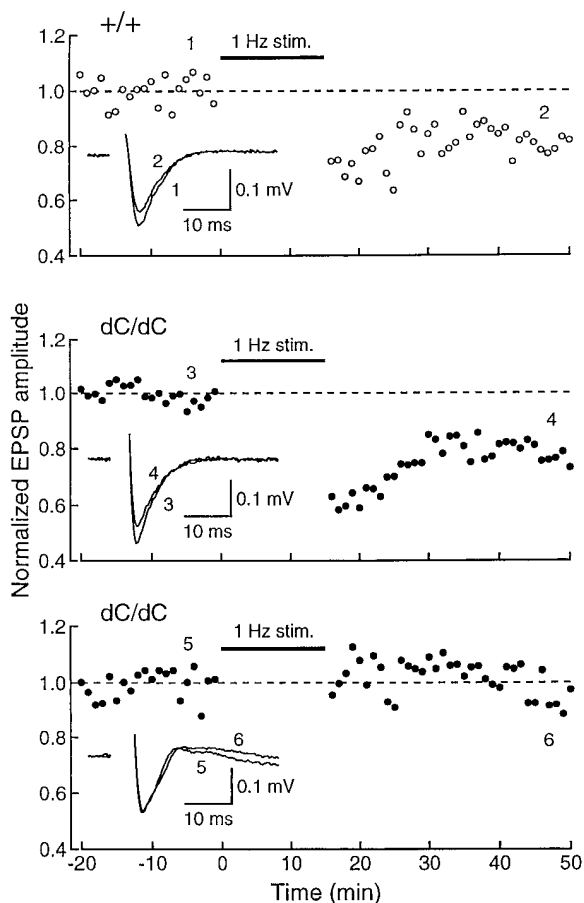
Figure 7. LTD in the CA1 Subfield of the Hippocampus

Examples of LTD in wild-type (+/+) (top) and mutant (dC/dC) (middle and bottom) mice at P2*–P3*. Afferent fibers were stimulated with a bipolar tungsten electrode at 0.1 Hz. Bars indicate prolonged low frequency stimulations (1 Hz for 15 min). Inleted traces represent averages of 10 consecutive EPSPs obtained at the times indicated. Each point on the graphs is the averaged amplitude of six consecutive responses. The broken lines on the panels indicate the average value of the EPSP amplitude during the control period.

GluRε2dC mutant mice and wild-type littermates derived from F2 mice were used for the following analyses, which were done in a blind fashion.

Breeding and maintenance of mice were carried out under institutional guidelines. Rearing by hand feeding of the neonatal mice was done as previously described (Kutsuwada et al., 1996), except that infant formula for human neonates, Neomilk L.ai (Snow Bland), was used.

Analyses of DNA and RNA

Southern blot analysis of tail DNA was done using the 0.5 kb SacI-BspHI fragment (probe A) from the genomic *GluRε2* clone, the 0.6 kb PstI fragment (probe Neo) from pGK2Neo, and the 0.34 kb Bpu1102I-XbaI fragment (probe B) from pSPGRε2 (Yamakura et al., 1993) as probes. PCR analysis was done with KOD Dash DNA polymerase (Toyobo) with primers 5'-GACACCTTCGTGGACCTGCAGAAGGAG GAG-3' (P1), 5'-GGCCGGGAAGTCCGGCCTTGTTTTCGACGC-3' (P2), and 5'-TCGTGCTTTACGGTATCGCCGCTCCCGATT-3' (P3).

RNase protection assay was performed according to the manufacturer's protocol with MAXIscript and HybSpeed kits (Ambion). Briefly, ~150,000 cpm of ^{32}P-labeled RNA antisense to nucleotide residues 2791–3093 of *GluRε2* mRNA (Kutsuwada et al., 1992) (probe
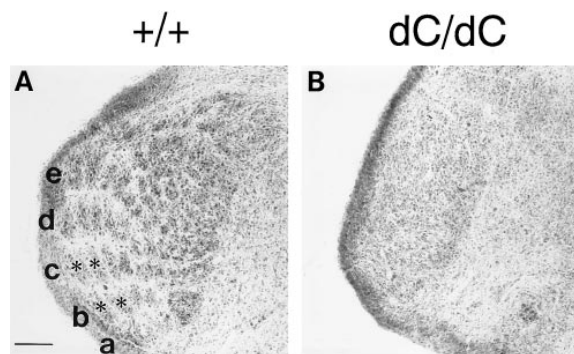

Figure 8. Barrelette Structures in the Brainstem Trigeminal Complex

Cytochrome oxidase histochemistry for whisker-related barrelette structures in the trigeminal spinal tract nucleus (subnucleus interpolaris) of wild-type (+/+) (A) and mutant (dC/dC) (B) mice at P2*. Five distinct rows (a–e) of patches (barrelette, asterisk) corresponding to whiskers are present in the wild-type trigeminal nucleus but are absent in the mutant trigeminal nucleus. Scale bar, 100 μm.

C) was incubated with 20 μg of total RNA prepared from the whole brain of mice at P0. The reaction products were analyzed on a 5% acrylamide/8 M urea gel. The gel was dried and exposed to X-ray film.

Western Blot Analysis

Whole brain homogenates were prepared from mice at P0 as described (Takahashi et al., 1996). The proteins (100 μg) were fractionated by SDS-PAGE and electroblotted onto a nitrocellulose membrane (Schleicher & Schuell). The blots were immunoreacted with purified anti-GluRε1C, anti-GluRε2N, anti-GluRε2C, and anti-GluRζ1N antibodies prepared by Watanabe et al. (1998) and with anti-GluR1, anti-GluR2/GluR3, and anti-GluR4 antibodies purchased from UBI at the concentration of 1 μg/ml. Immunoreacted protein bands were visualized by chemiluminescence (ECL detection system, Amersham). For quantitation, the bands were scanned by a computing densitometer (Gel Documentation System, UVP) and analyzed with NIH Image software (version 1.58).

Histology

Mice at P2* were fixed transcardially with 4% paraformaldehyde and 0.2% picrinic acid in 0.1 M sodium phosphate buffer (pH 7.4) (PB). Brains were postfixed in the same fixative for an additional 2–3 hr at 4°C and dipped in PB containing 30% sucrose for 1–2 days.

For cytochrome oxidase histochemistry, coronal sections (30 μm) through the subnucleus interpolaris of the trigeminal spinal tract nucleus were prepared by cryostat and mounted on gelatin-coated glass slides. Sections were incubated for 10–12 hr at 37°C in PB containing 0.3 mg/ml cytochrome c (Sigma), 0.5 mg/ml diaminobenzidine (Sigma), and 45 mg/ml sucrose (Wong-Riley, 1979). Photographs were taken with an Olympus AX80 light microscope.

Immunofluorescence staining was carried out with rabbit anti-mouse GluRε2N antibody raised against N-terminal polypeptide of the mouse GluRε2 subunit (Watanabe et al., 1998) and with guinea pig anti-mouse synaptophysin antibody raised against amino acid residues 205–259, which recognized a single band of 38 kDa in immunoblots of mouse brain proteins (Yamada et al., personal communication). Fixed brains were embedded in paraffin wax to prepare coronal sections through the hippocampus (5 μm in thickness). Sections were treated at 37°C for 10 min with 0.1–0.3 μg/ml pepsin (DAKO) in 0.2 N HCl. After blocking with 10% normal goat serum, sections were incubated overnight with anti-GluRε2N antibody (0.2 μg/ml), followed by incubations with biotinylated goat anti-rabbit IgG for 1 hr and streptavidin-peroxidase for 30 min (Histofine SAB-PO(R) Kit; Nichirei, Japan). The first immunoreaction was visualized with the Tyramide Signal Amplification Kit (TSATM-DIRECT [GREEN],

NEN). Then, sections were incubated overnight with anti-synaptophysin antibody (0.5 μg/ml) and visualized with Cy3–donkey anti–guinea pig IgG (Jackson Immunoresearch) for 2 hr. Photographs were taken by a confocal laser scanning microscope (MRC 1024, BioRad).

Cell Culture and Immunocytochemistry

Cultures of cerebral neurons were prepared from 18-day-old embryonic mice as described (Bartlett and Banker, 1984). Briefly, cells from the dissected cerebrum were dissociated by trypsin (0.25%) and trituration and were plated on poly-L-lysine–coated glass coverslips in minimal essential medium (MEM) with 10% horse serum at a density of 2×10^6 cells per 35 mm dish. After the attachment of cells, the coverslips were transferred and the neurons were maintained in serum-free MEM with N-2 supplement (Gibco/BRL), 2-mercaptoethanol (10 μM), ovalbumin (0.1%), and pyruvate (0.01 mg/ml). Cytosine arabinoside (5 μM) was added after 2 days to inhibit glial proliferation. The neurons cultured for 4 or 7 days were fixed with methanol for 10 min at $-20°C$, and immunocytochemical staining was carried out as above with rabbit anti-mouse GluRε2N antibody, guinea pig anti-mouse GluRα1 antibody (Watanabe et al., 1998), guinea pig anti-mouse synaptophysin antibody, and monoclonal mouse anti-synaptophysin antibody (ICN Biomedicals). Photographs were taken by a confocal laser scanning microscope (MRC 600, BioRad).

Electrophysiology

Electrophysiological analyses of synaptic transmission and LTD in hippocampal slices were done as described (Kutsuwada et al., 1996). Single channel recordings from hippocampal CA1 pyramidal cells were made from membrane patches in the outside-out configuration using an Axopatch-1D (Axon Instruments) amplifier. The pipette solution contained (in mM): Cs gluconate 122.5, CsCl 17.5, Cs-HEPES 10, EGTA 0.2, NaCl 8, Mg-ATP 2, and Na_3-GTP 0.3 (pH 7.3 with CsOH). The external solution contained (in mM): NaCl 119, KCl 2.5, $CaCl_2$ 2.5, NaH_2PO_4 1, $NaHCO_3$ 26.2, and glucose 11 and had been pregassed with 95% O_2 and 5% CO_2. Single channel currents were activated by 50 μM NMDA in nominally Mg^{2+}-free solution containing 100 μM picrotoxin and 0.3 μM tetrodotoxin. Currents were recorded on digital audio tape (Sony PC204A) and analyzed offline. Records were filtered at 2 kHz (eight-pole Bessel filter) and digitized at 20 kHz (Dagan LM-12S Interface). Only openings longer than two filter rise times (332 μs) were analyzed (Colquhoun and Sigworth, 1995). The channel openings with subconductance levels were not analyzed in this study. Mean conductances were determined from the maximum likelihood of fits of Gaussian distribution. Open time distributions, which comprise only the duration of single openings, were analyzed. Histograms were binned logarithmically, and a square root transformation of the ordinate (event per bin) was used. Exponential functions were fitted by the maximum likelihood method (Colquhoun and Sigworth, 1995). Plotted in this way, peaks correspond to the time constant of the exponential (Sigworth and Sine, 1987).

References

Akazawa, C., Shigemoto, R., Bessho, Y., Nakanishi, S., and Mizuno, N. (1994). Differential expression of five N-methyl-D-aspartate receptor subunit mRNAs in the cerebellum of developing and adult rats. J. Comp. Neurol. *347*, 150–160.

Aoki, C., Venkatesan, C., Go, C.G., Mong, J.A., and Dawson, T.M.

(1994). Cellular and subcellular localization of NMDA-R1 subunit immunoreactivity in the visual cortex of adult and neonatal rats. J. Neurosci. *14*, 5202–5222.

Bartlett, W.P., and Banker, G.A. (1984). An electron microscopic study of the development of axons and dendrites by hippocampal neurons in culture. I. Cells, which develop without intercellular contacts. J. Neurosci. *4*, 1944–1953.

Bliss, T.V.P., and Collingridge, G.L. (1993). A synaptic model of memory: long-term potentiation in the hippocampus. Nature *361*, 31–39.

Buckley, K.M., Floor, E., and Kelly, R.B. (1987). Cloning and sequence analysis of cDNA encoding p38, a major synaptic vesicle protein. J. Cell Biol. *105*, 2447–2456.

Chevesich, J., Kreuz, A.J., and Montell, C. (1997). Requirement for the PDZ domain protein, INAD, for localization of the TRP store–operated channel to a signaling complex. Neuron *18*, 95–105.

Cline, H.T., Debski, E.A., and Constantine-Paton, M. (1987). N-methyl-D-aspartate receptor antagonist desegregates eye-specific stripes. Proc. Natl. Acad. Sci. USA *84*, 4342–4345.

Colquhoun, D., and Sigworth, F.J. (1995). Fitting and statistical analysis of single- channel records. In Single-Channel Recording, Second Edition, B. Sakmann and E. Neher, eds. (New York: Plenum), pp. 483–587.

Cummings, J.A., Mulkey, R.M., Nicoll, R.A., and Malenka, R.C. (1996). Ca^{2+} signaling requirements for long-term depression in the hippocampus. Neuron *16*, 825–833.

DeChiara, T.M., Bowen, D.C., Valenzuela, D.M., Simmons, M.V., Poueymirou, W.T., Thomas, S., Kinetz, E., Compton, D.L., Rojas, E., Park, J.S., et al. (1996). The receptor tyrosine kinase MuSK is required for neuromuscular junction formation in vivo. Cell *85*, 501–512.

Ebralidze, A.K., Rossi, D.J., Tonegawa, S., and Slater, N.T. (1996). Modification of NMDA receptor channels and synaptic transmission by targeted disruption of the NR2C gene. J. Neurosci. *16*, 5014–5025.

Ehlers, M.D., Tingley, W.G., and Huganir, R.L. (1995). Regulated subcellular distribution of the NR1 subunit of the NMDA receptor. Science *269*, 1734–1737.

Forrest, D., Yuzaki, M., Soares, H.D., Ng, L., Luk, D.C., Sheng, M., Stewart, C.L., Morgan, J.I., Connor, J.A., and Curran, T. (1994). Targeted disruption of NMDA receptor 1 gene abolishes NMDA response and results in neonatal death. Neuron *13*, 325–338.

Hollmann, M., Boulter, J., Maron, C., Beasley, L., Sullivan, J., Pecht, G., and Heinemann, S. (1993). Zinc potentiates agonist-induced currents at certain splice variants of the NMDA receptor. Neuron *10*, 943–954.

Ikeda, K., Nagasawa, M., Mori, H., Araki, K., Sakimura, K., Watanabe, M., Inoue, Y., and Mishina, M. (1992). Cloning and expression of the ε4 subunit of the NMDA receptor channel. FEBS Lett. *313*, 34–38.

Ikeda, K., Araki, K., Takayama, C., Inoue, Y., Yagi, T., Aizawa, S., and Mishina, M. (1995). Reduced spontaneous activity of mice defective in the ε4 subunit of the NMDA receptor channel. Mol. Brain Res. *33*, 61–71.

Ito, I., Futai, K., Katagiri, H., Watanabe, M., Sakimura, K., Mishina, M., and Sugiyama, H. (1997). Synapse-selective impairment of NMDA receptor functions in mice lacking NMDA receptor ε1 or ε2 subunit. J. Physiol. *500*, 401–408.

Kadotani, H., Hirano, T., Masugi, M., Nakamura, K., Nakao, K., Katsuki, M., and Nakanishi, S. (1996). Motor discoordination results from combined gene disruption of the NMDA receptor NR2A and NR2C subunits, but not from single disruption of the NR2A or NR2C subunit. J. Neurosci. *16*, 7859–7867.

Kim, E., Cho, K.-O., Rothschild, A., and Sheng, M. (1996). Heteromultimerization and NMDA receptor–clustering activity of chapsyn-110, a member of the PSD-95 family of proteins. Neuron *17*, 103–113.

Kiyama, Y., Manabe, T., Sakimura, K., Kawakami, F., Mori, H., and Mishina, M. Increased thresholds for LTP and contextual learning in mice lacking the GluRε1 subunit of the NMDA receptor channel. J. Neurosci., in press.

Kleinschmidt, A., Bear, M.F., and Singer, W. (1987). Blockade of "NMDA" receptors disrupts experience-dependent plasticity of kitten striate cortex. Science *238*, 355–358.

Kornau, H.-C., Schenker, L.T., Kennedy, M.B., and Seeburg, P.H. (1995). Domain interaction between NMDA receptor subunits and the postsynaptic density protein PSD-95. Science 269, 1737–1740.

Kutsuwada, T., Kashiwabuchi, N., Mori, H., Sakimura, K., Kushiya, E., Araki, K., Meguro, H., Masaki, H., Kumanishi, T., Arakawa, M., et al. (1992). Molecular diversity of the NMDA receptor channel. Nature 358, 36–41.

Kutsuwada, T., Sakimura, K., Manabe, T., Takayama, C., Katakura, N., Kushiya, E., Natsume, R., Watanabe, M., Inoue, Y., Yagi, T., et al. (1996). Impairment of suckling response, trigeminal neuronal pattern formation, and hippocampal LTD in NMDA receptor ε2 subunit mutant mice. Neuron 16, 333–344.

Laurie, D.J., and Seeburg, P.H. (1994). Regional and developmental heterogeneity in splicing of the rat brain NMDAR1 mRNA. J. Neurosci. 14, 3180–3194.

Li, Y., Erzurumlu, R.S., Chen, C., Jhaveri, S., and Tonegawa, S. (1994). Whisker-related neuronal patterns fail to develop in the trigeminal brainstem nuclei of NMDAR1 knockout mice. Cell 76, 427–437.

Malenka, R.C., and Nicoll, R.A. (1993). NMDA-receptor–dependent synaptic plasticity: multiple forms and mechanisms. Trends Neurosci. 16, 521–527.

Meguro, H., Mori, H., Araki, K., Kushiya, E., Kutsuwada, T., Yamazaki, M., Kumanishi, T., Arakawa, M., Sakimura, K., and Mishina, M. (1992). Functional characterization of a heteromeric NMDA receptor channel expressed from cloned cDNAs. Nature 357, 70–74.

Monyer, H., Sprengel, R., Schoepfer, R., Herb, A., Higuchi, M., Lomeli, H., Burnashev, N., Sakmann, B., and Seeburg, P.H. (1992). Heteromeric NMDA receptors: molecular and functional distinction of subtypes. Science 256, 1217–1221.

Monyer, H., Burnashev, N., Laurie, D.J., Sakmann, B., and Seeburg, P.H. (1994). Developmental and regional expression in the rat brain and functional properties of four NMDA receptors. Neuron 12, 529–540.

Moon, I.S., Apperson, M.L., and Kennedy, M.B. (1994). The major tyrosine-phosphorylated protein in the postsynaptic density fraction is N-methyl-D-aspartate receptor subunit 2B. Proc. Natl. Acad. Sci. USA 91, 3954–3958.

Mori, H., and Mishina, M. (1995). Structure and function of the NMDA receptor channel. Neuropharmacology 34, 1219–1237.

Mori, H., Yamakura, T., Masaki, H., and Mishina, M. (1993). Involvement of the carboxy-terminal region in modulation by TPA of the NMDA receptor channel. NeuroReport 4, 519–522.

Moriyoshi, K., Masu, M., Ishii, T., Shigemoto, R., Mizuno, N., and Nakanishi, S. (1991). Molecular cloning and characterization of the rat NMDA receptor. Nature 354, 31–37.

Müller, B.M., Kistner, U., Kindler, S., Chung, W.J., Kuhlendahl, S., Fenster, S.D., Lau, L.-F., Veh, R.W., Huganir R.L., Gundelfinger, E.D., et al. (1996). SAP102, a novel postsynaptic protein that interacts with NMDA receptor complexes in vivo. Neuron 17, 255–265.

Nagasawa, M., Sakimura, K., Mori, K.J., Bedell, M.A., Copeland, N.G., Jenkins, N.A., and Mishina, M. (1996). Gene structure and chromosomal localization of the mouse NMDA receptor channel subunits. Mol. Brain Res. 36, 1–11.

Niethammer, M., Kim, E., and Sheng, M. (1996). Interaction between the C terminus of NMDA receptor subunits and multiple members of the PSD-95 family of membrane-associated guanylate kinases. J. Neurocsi. 16, 2157–2163.

Omkumar, R.V., Kiely, M.J., Rosenstein, A.J., Min, K.T., and Kennedy, M.B. (1996). Identification of a phosphorylation site for calcium/calmodulin dependent protein kinase II in the NR2B subunit of the N-methyl-D-aspartate receptor. J. Biol. Chem. 271, 31670–31678.

Sakimura, K., Kutsuwada, K., Ito, I., Manabe, T., Takayama, C., Kushiya, E., Yagi, T., Aizawa, S., Inoue, Y., Sugiyama, H., et al. (1995). Reduced hippocampal LTP and spatial learning in mice lacking NMDA receptor ε1 subunit. Nature 373, 151–155.

Schmechel, D., Marangos, P.J., Zis, A.P., Brighman, M., and Goodwin, F.K. (1978). Brain enolase as specific markers of neuronal and glial cells. Science 199, 313–315.

Seeburg, P.H. (1993). The molecular biology of mammalian glutamate receptor channels. Trends Neurosci. 16, 359–365.

Sigworth, F.J., and Sine, S.M. (1987). Data transformations for improved display and fitting of single-channel dwell time histograms. Biophys. J. 52, 1047–1054.

Simske, J.S., Keach, S.M., Harp, S.A., and Kim, S.K. (1996). LET-23 receptor localization by the cell junction protein LIN-7 during C. elegans vulval induction. Cell 85, 195–204.

Sprengel, R., Suchanek, B., Amico, C., Brusa, R., Burnashev, N., Rozov, A., Hvalby, Ø., Jensen, V., Paulsen, O., Andersen, P., et al. (1998). Importance of the intracellular domain of NR2 subunits for NMDA receptor function in vivo. Cell 92, 279–289.

Sternberg, N., Sauer, B., Hoess, R., and Abremski, K. (1986). Bacteriophage P1 cre gene and its regulatory region. J. Mol. Biol. 187, 197–212.

Sugihara, H., Moriyoshi, K., Ishii, T., Masu, M., and Nakanishi, S. (1992). Structures and properties of seven isoforms of the NMDA receptor generated by alternative splicing. Biochem. Biophys. Res. Commun. 185, 826–832.

Takahashi, T., Feldmeyer, D., Suzuki, N., Onodera, K., Cull-Candy, S.G., Sakimura, K., and Mishina, M. (1996). Functional correlation of NMDA receptor ε subunits expression with the properties of single-channel and synaptic currents in the developing cerebellum. J. Neurosci. 16, 4376–4382.

Tejedor, F.J., Bokhari, A., Rogero, O., Gorczyca, M., Zhang, J., Kim, E., Sheng, M., and Budnik, V. (1997). Essential role for dlg in synaptic clustering of Shaker K⁺ channels in vivo. J. Neurosci. 17, 152–159.

Watanabe, M., Inoue, Y., Sakimura, K., and Mishina, M. (1992). Developmental changes in distribution of NMDA receptor channel subunit mRNAs. NeuroReport 3, 1138–1140.

Watanabe, M., Inoue, Y., Sakimura, K., and Mishina, M. (1993). Distinct distributions of five N-methyl-D-aspartate receptor channel subunit mRNAs in the forebrain. J. Comp. Neurol. 338, 377–390.

Watanabe, M., Fukaya, M., Sakimura, K., Manabe, T., Mishina, M., and Inoue, Y. (1998). Selective scarcity of NMDA receptor channel subunits in the stratum lucidum (mossy fiber–recipient layer) of the mouse hippocampal CA3 subfield. Eur. J. Neurosci. 10, 478–487.

Wong-Riley, M. (1979). Changes in the visual system of monocularly sutured or enucleated cats demonstrable with cytochrome oxidase histochemistry. Brain Res. 171, 11–28.

Wyszynski, M., Lin, J., Rao, A., Nigh, E., Beggs, A.H., Craig, A.M., and Sheng, M. (1997). Competitive binding of α-actinin and calmodulin to the NMDA receptor. Nature 385, 439–442.

Yagi, T., Tokunaga, T., Furuta, Y., Nada, S., Yoshida, M., Tsukada, T., Saga, Y., Takeda, N., Ikawa, Y., and Aizawa, S. (1993a). A novel ES cell line, TT2, with high germline-differentiating potency. Anal. Biochem. 214, 70–76.

Yagi, T., Nada, S., Watanabe, N., Tamemoto, H., Kohmura, N., Ikawa, Y., and Aizawa, S. (1993b). A novel negative selection for homologous recombinants using diphtheria toxin A fragment gene. Anal. Biochem. 214, 77–86.

Yamakura, T., Mori, H., Shimoji, K., and Mishina, M. (1993). Phosphorylation of the carboxy-terminal domain of the ζ1 subunit is not responsible for potentiation by TPA of the NMDA receptor channel. Biochem. Biophys. Res. Commun. 196, 1537–1544.

Yamazaki, M., Mori, H., Araki, K., Mori, K.J., and Mishina, M. (1992). Cloning, expression and modulation of a mouse NMDA receptor subunit. FEBS Lett. 300, 39–45.

Zhong, J., Carrozza, D.P., Williams, K., Pritchett, D.B., and Molinoff, P.B. (1995). Expression of mRNAs encoding subunits of the NMDA receptor in developing rat brain. J. Neurochem. 64, 531–539.